

# Experimental investigation of deformations of a premixed methane/air flame in a turbulent swirling jet

Aleksei S. Lobasov\*<sup>1,2</sup>, Sergey S. Abdurakipov<sup>1,2</sup>, Leonid M. Chikishev<sup>1,2</sup>, Vladimir M. Dulin<sup>1,2</sup>,  
Dmitriy M. Markovich<sup>1,2</sup>

<sup>1</sup> Kutateladze Institute of Thermophysics, 1 Ak. Lavrentyeva Avenue, 630090, Novosibirsk,  
Russia

<sup>2</sup> Novosibirsk State University, 2 Pirogova Street, 630090, Novosibirsk, Russia

\*phone: +7-383-3325678, e-mail: [Alexey.Lobasov@gmail.com](mailto:Alexey.Lobasov@gmail.com)

**Abstract:** The paper reports on results of the experimental study of spatial structure of preheat zone in turbulent methane/air swirling jet-flames at atmospheric pressure. The Reynolds number based on the flowrate and viscosity of the air was fixed as 5 000. Swirl rate  $S$  of the flow exceeded a critical value for breakdown of the swirling jet's vortex core and formation of the recirculation zone at the jet axis. The spatial structure of the flame was investigated by planar laser-induced fluorescence of formaldehyde (HCHO PLIF). Three cases of the equivalence ratio  $\phi$  of the mixture issuing from the nozzle-burner were considered, viz., 0.7, 1.4 and 2.5. The latter case corresponded to a lifted flame of fuel-rich swirling jet flow partially premixed with the surrounding air. PLIF snapshots, captured almost instantaneously, revealed two different kinds of the reaction zone deformations, viz., small-scale instabilities of the flame front and large-scale deformations, induced by the unsteady flow dynamics. To extract information about the coherent structures of the flame deformation, a principal component analysis (PCA) has been applied. The analysis revealed that the largest structural deformations correspond to nearly-axisymmetric oscillations, expected to be caused by the buoyancy force. Another coherent structure is an asymmetric mode, presumably induced by large-scale vortex structures detected in the previous study of fuel-rich lifted flame [1].

**Key words:** turbulent swirling flame, unsteady flame dynamics, planar laser-induced fluorescence, principle component analysis.

## 1. Introduction

Swirl is often used for stabilization of jet-flames. Jet flows with strong swirl are featured by breakdown of the swirling vortex core, formation of the central recirculation zone and presence of spiral/helical vortices [2]. Effect of such flow features as vortex breakdown and precession of the vortex core on the combustion in swirling jets is still not completely understood. In particular, impact of the large-scale vortex structures (including precessing vortex core, see [1, 3]) on dynamics and stability of flames in swirling flows is still a debated issue [4]. Thus, analysis of flame-vortex interactions in swirl-stabilized combustors is important for better understanding of unsteady combustion phenomena [5].

The large-scale vortices are known to induce deformations of the flame front, affect heat release rate and can result in local flame extinction. These features have been recently studied by using combination of particle image velocimetry and planar-laser induced fluorescence (PLIF) of hydroxyl [6,7], produced in the flame front and present in the combustion products. Snapshot proper orthogonal decomposition [8] (or PCA) was applied to PIV data to extract coherent structures, similarly to [1,2] for the non-reacting and reacting strongly swirling jets with vortex breakdown. Stöhr et al. [6] have found that large-scale vortices improve mixing between the combustion products and fresh mixture. Meanwhile, Boxx et al. [7] observed events of local flame extinction during interaction with large-scale vortices, formed in the high-swirl flow. Nevertheless, a detailed analysis of the reaction zone shape and flame front deformations,

including those, which are not induced directly by large-scale flow motions, is desirable.

Formaldehyde (HCHO) is an important combustion intermediate occurring in lower-temperature regions of hydrocarbon-fueled flames. It plays an important role in several combustion processes, including fuel oxidation, auto-ignition, lifted-flame stabilization. It is the initial step of the  $\text{HCHO} \rightarrow \text{HCO} \rightarrow \text{CO}$  oxidation pathway of conventional hydrocarbons [9]. High concentration of HCHO specify preheat zone of hydrocarbon flames. Photochemical properties of HCHO are well studied [10]. One of the more prevalent strategies for HCHO PLIF measurements is the excitation of transition by using third harmonic of Nd:YAG laser radiation at 355 nm [11, 12]. Despite of the low intensity of the sideband transition excited near 355 nm, energy of the commercially available pulsed Nd:YAG lasers allows to reach high enough fluorescence signal and allow PLIF measurements without using a specific tunable laser.

The present paper reports on combustion regimes of methane/air mixture in a high-swirl turbulent jet, featured by the vortex breakdown and presence of the central recirculation zone [1], by using HCHO PLIF. The focus is placed on large-scale deformation of the reaction zone by using PCA.

## **2. Experimental setup and measurements techniques**

The flames were organized in an open combustion rig (see details in [1]) with a burner, made of a contraction axisymmetric nozzle (with the exit diameter of  $d = 15$  mm) with a vane swirl installed inside (see Figure 1). The swirl rate based

on definition in [2] was 1.0, which is well above the critical value of 0.6 for the vortex breakdown. Three cases of the equivalence ratio  $\phi$  of methane/air mixture issued from the nozzle were studied 0.7, 1.4 and 2.5. The jet Reynolds number, based on the flowrate and viscosity of the air was fixed as 5 000. The jet bulk velocity without fuel flow was  $U_0 = 5$  m/s.

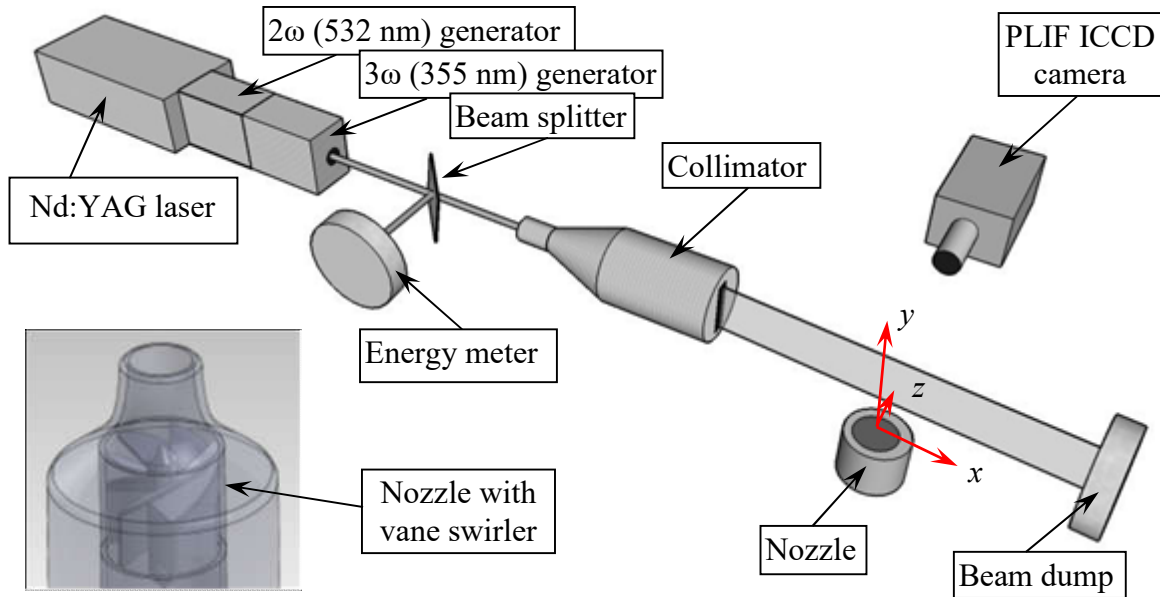


Figure 1. Sketch of the PLIF setup

The layout of the PLIF setup is shown in Figure 1. The PLIF measurements were carried out for the longitudinal cross-plane and for transverse cross-planes (parallel and perpendicular to the jet axis, respectively) of the flow for different distances from the burner rim. The distances from the burner rim to the measurement plane were varied by moving the former one along the vertical axis. A motorized traversing system with accuracy of  $100 \mu\text{m}$  was used.

Radiation of the third harmonic (355nm) of a Nd:YAG laser (Quantel Brilliant B with 45 mJ energy per pulse) has been used for excitation of HCHO fluorescence. The A–X transition was excited. RMS of the laser pulses energy

variation was below 5%. A collimator optics was used to obtain the light sheet of 50 mm width with thickness below 0.8 mm in the measurement region. The fluorescence of HCHO was collected by a 16-bit sCMOS camera LaVision Imager Pro X equipped with an IRO unit, UV Lens (f#2.8) and HCHO PLIF optical filter. The exposure time for each image was 200 ns. The raw PLIF images were corrected accounting for non-uniform intensity of the laser sheet, shot-to-shot variations of the laser energy, non-uniform sensitivity of the sensor. Background signal was also subtracted.

To reveal intensive coherent structures in the PLIF images, the PCA was applied to the ensembles of  $N = 1000$  PLIF snapshots for each type of the flame. The PCA was implemented via the singular value decomposition method [13]:

$$c'(x, y, t_k) = \sum_{q=1}^{N-1} \alpha_q(t_k) \sigma_q \varphi_q(x, y), \quad (1)$$

$$\text{where } \int_{\Omega_{xy}} \varphi_i \varphi_j dx dy = \delta_{ij} \text{ and } \frac{1}{N} \sum_{k=1}^N \alpha_i(t_k) \alpha_j(t_k) = \delta_{ij}. \quad (2)$$

$\delta_{ij}$  is the Kronecker delta.

### 3. Results

Figure 2 shows photographs of the flames and examples of the HCHO PLIF data. The PLIF snapshots provide information about spatial structure of preheat zones, for the longitudinal plane. The grayscale is fixed for all PLIF images.

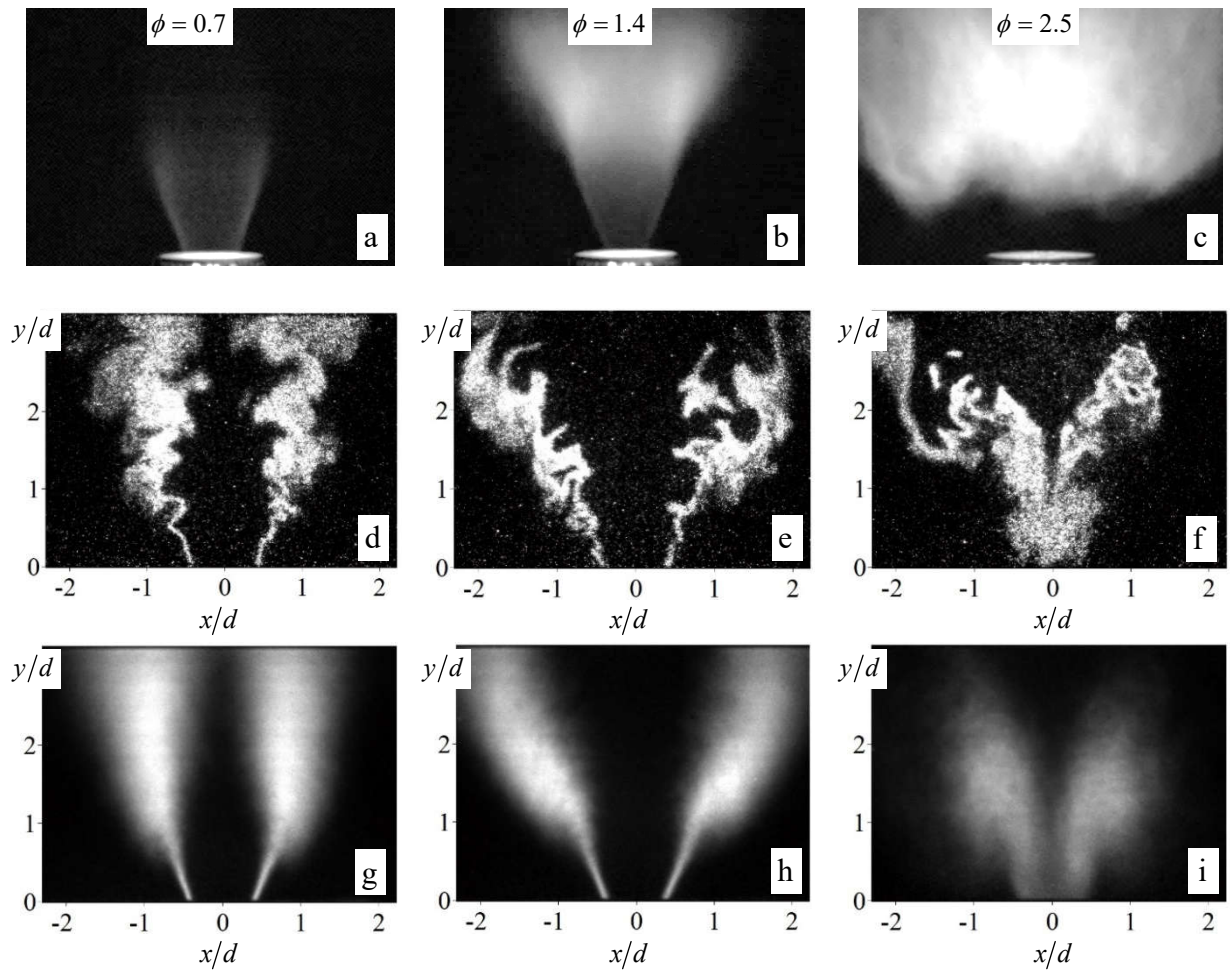


Figure 2. (a-c) Direct images of the flames and the (d-f) instantaneous and (g-i) time-averaged HCHO PLIF signal

On average, flame for the fuel-lean mixture with  $\phi = 0.7$  and fuel-rich mixture with  $\phi = 1.4$  has shape of an inverted cone. According to the instantaneous snapshots, the reaction zone is subjected to deformations which become larger downstream. Moreover, separated islands are detected in several instantaneous patterns. These observations may originate from two different conditions: out-of-plane closing of the reaction zones or combustion in detached zones, including those trapped by large-scale vortices. Shape of the reacting zone in case of the fuel-rich lifted flame with  $\phi = 2.5$  (stabilized at a certain distance downstream the burner rim) is different from the two other cases. In particular, one can observe

HCHO fluorescence around the jet axis for  $y/d$  typically below one. Figure 3 shows PCA spectra for the PLIF data for the longitudinal plane. For the fuel-rich lifted flame, the amplitude of the first PCA mode is considerably greater than amplitude of each other mode (more than twice for  $i > 2$ ).

Spatial distributions of the first four PCA modes are shown in Figure 4. For the fuel-lean flame the first mode corresponds to oscillations of the PLIF intensity along the mixing layer. Shape of the mode appears to be roughly symmetrical with respect to the  $y$ -axis. The second and third PCA modes correspond to spatial deformations of traveling waves along the flame, which are similar with respect to the phase shift of  $\pi/2$ . The distributions of the PLIF intensity oscillations correspond to anti-symmetrical deformations of the reaction zone. The PCA modes for the fuel-rich flame with  $\phi = 1.4$  also correspond to symmetrical and asymmetrical modes of the reaction zone deformations which become greater downstream.

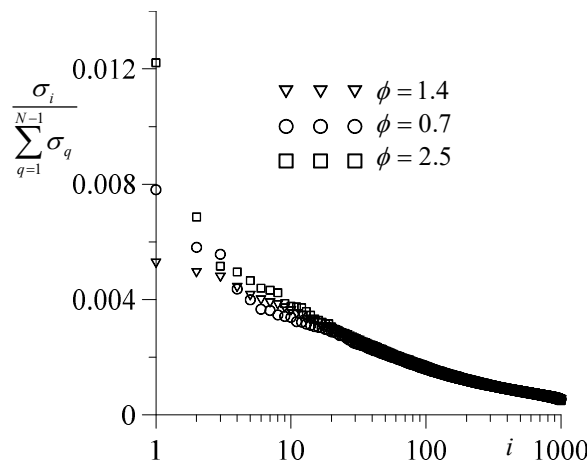


Figure 3. PCA spectra for PLIF data for the longitudinal plane of the swirling methane/air flames

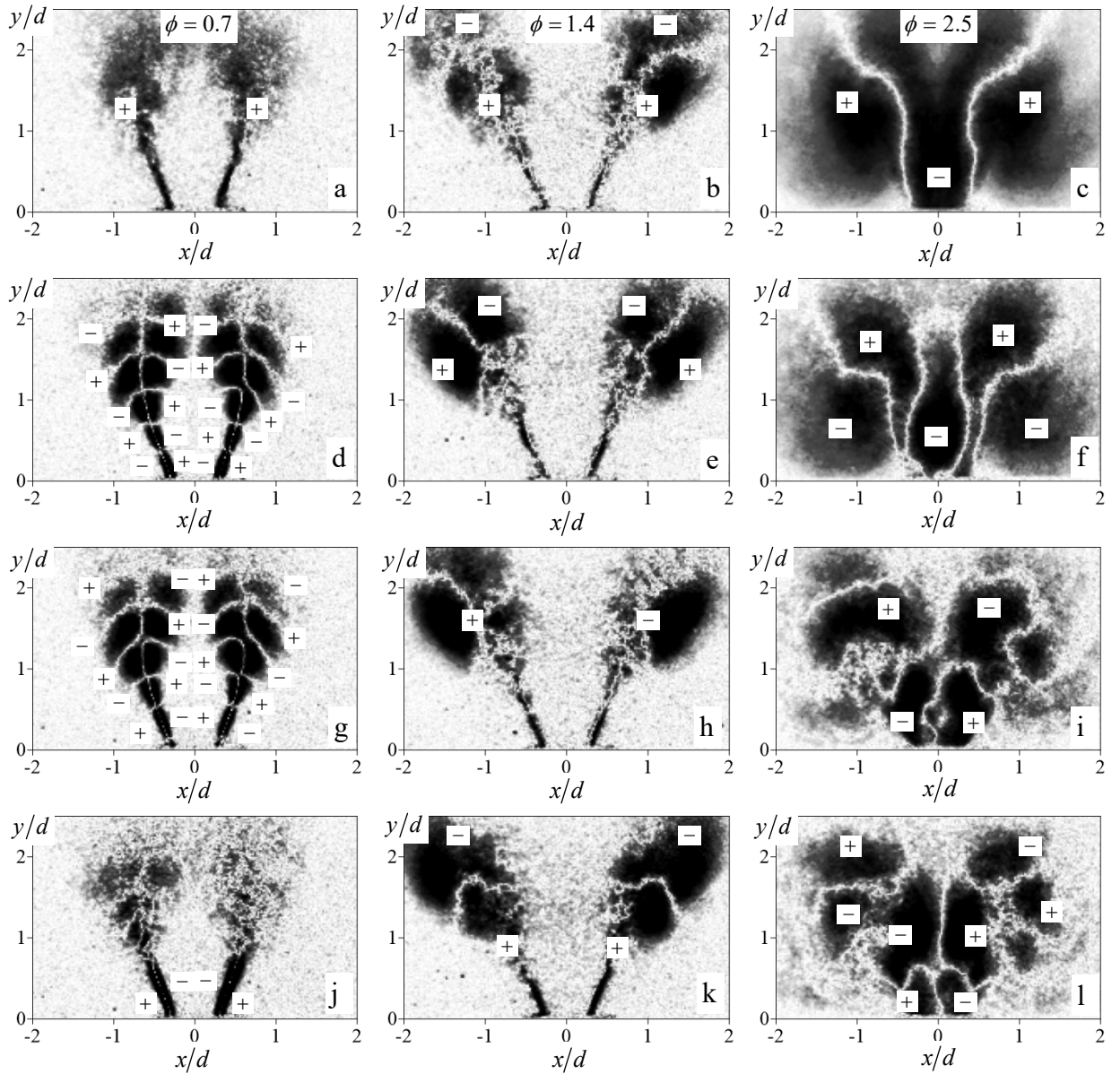


Figure 4. Spatial distributions of the first four PCA modes (a-c)  $\phi_1$ , (d-f)  $\phi_2$ , (g-i)  $\phi_3$ , (j-l)  $\phi_4$  for HCHO PLIF data for the longitudinal plane of the swirling methane/air flames for (a,d,g,j)  $\phi = 0.7$ , (b,e,h,k)  $\phi = 1.4$ , (c,f,i,l)  $\phi = 2.5$

The first two PCA modes for the fuel-rich lifted flame with  $\phi = 2.5$  correspond to large-scale symmetrical oscillations of the PLIF intensity around the  $y$ -axis and in the mixing layer between the jet and surrounding air. The third and



fourth PCA modes correspond to disturbances in a form of traveling waves along the jet with asymmetric form with respect to the  $y$ -axis.

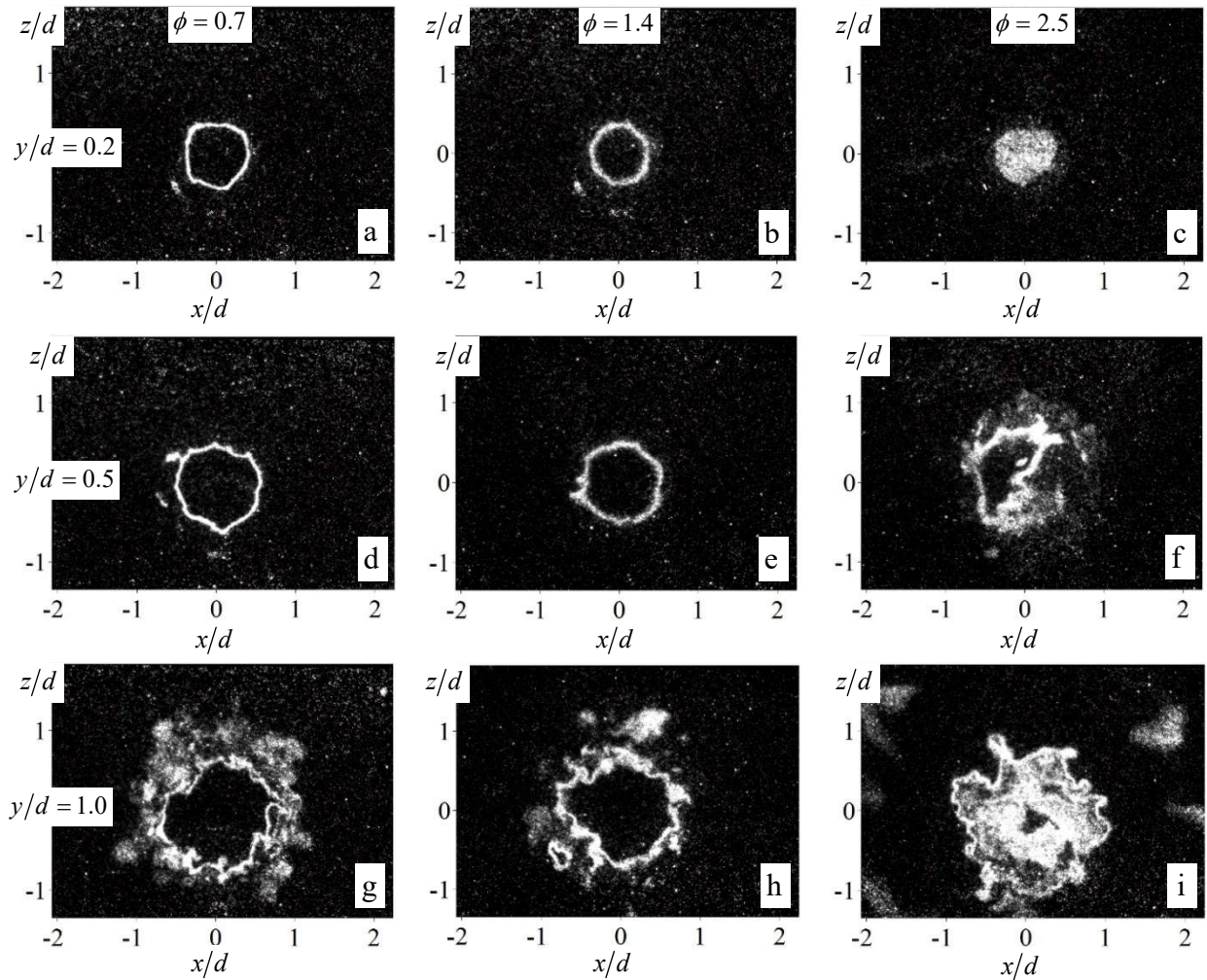


Figure 5. Examples of the instantaneous HCHO PLIF signal for the transverse cross-planes (a-c)  $y/d = 0.2$ , (d-f)  $y/d = 0.5$ , (g-i)  $y/d = 1.0$  of the swirling methane/air flames for (a,d,g)

$$\phi = 0.7, (b,e,h) \phi = 1.4, (c,f,i) \phi = 2.5$$

Examples of the HCHO PLIF data captured at transverse cross-planes for three different distances from the nozzle are shown in Figure 5. The example for  $y/d = 0.2$  for the case with  $\phi = 2.5$  confirms presence of the reaction zone at the jet axis. In general, for all cases surface of the reaction zone is not axisymmetric and subjected to deformations. Deformations increase in size downstream from the

burner. Besides, presence of isolated smaller reaction zones can be seen in the transverse cross-planes.

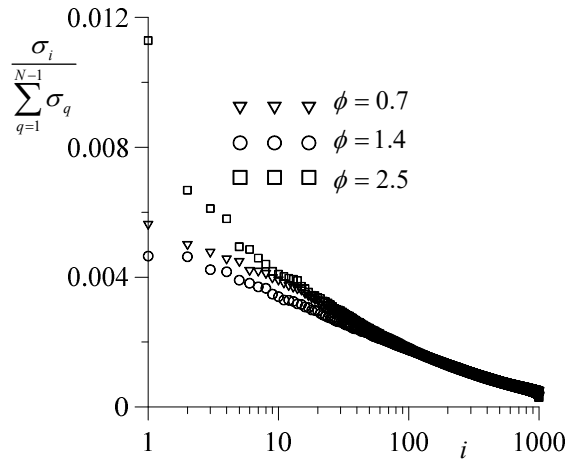


Figure 6. PCA spectra for PLIF data for the transverse cross-section  $y/d = 1.5$  of the swirling methane/air flames

PCA spectrum for the PLIF images for the transverse cross-section  $y/d = 1.5$  are shown in Figure 6. The highest amplitude corresponds to the first PCA mode for the fuel-rich lifted flame with  $\phi = 2.5$ . According to the spatial distribution shown in Figure 7, this mode corresponds to axisymmetric mode of the reaction zone deformations. For the cases with  $\phi = 0.7$  and  $\phi = 1.4$ , the first PCA mode also corresponds to the reaction zone oscillations with almost axisymmetric mode. The second and third PCA modes for the case  $\phi = 2.5$  correspond to a rotating coherent structure, similar to that observed in [6]. Notably, that the second and third PCA modes for each flame (for the considered region) appear to represent coherent structure with respect to rotation by  $90^\circ$  around the  $y$ -axis.

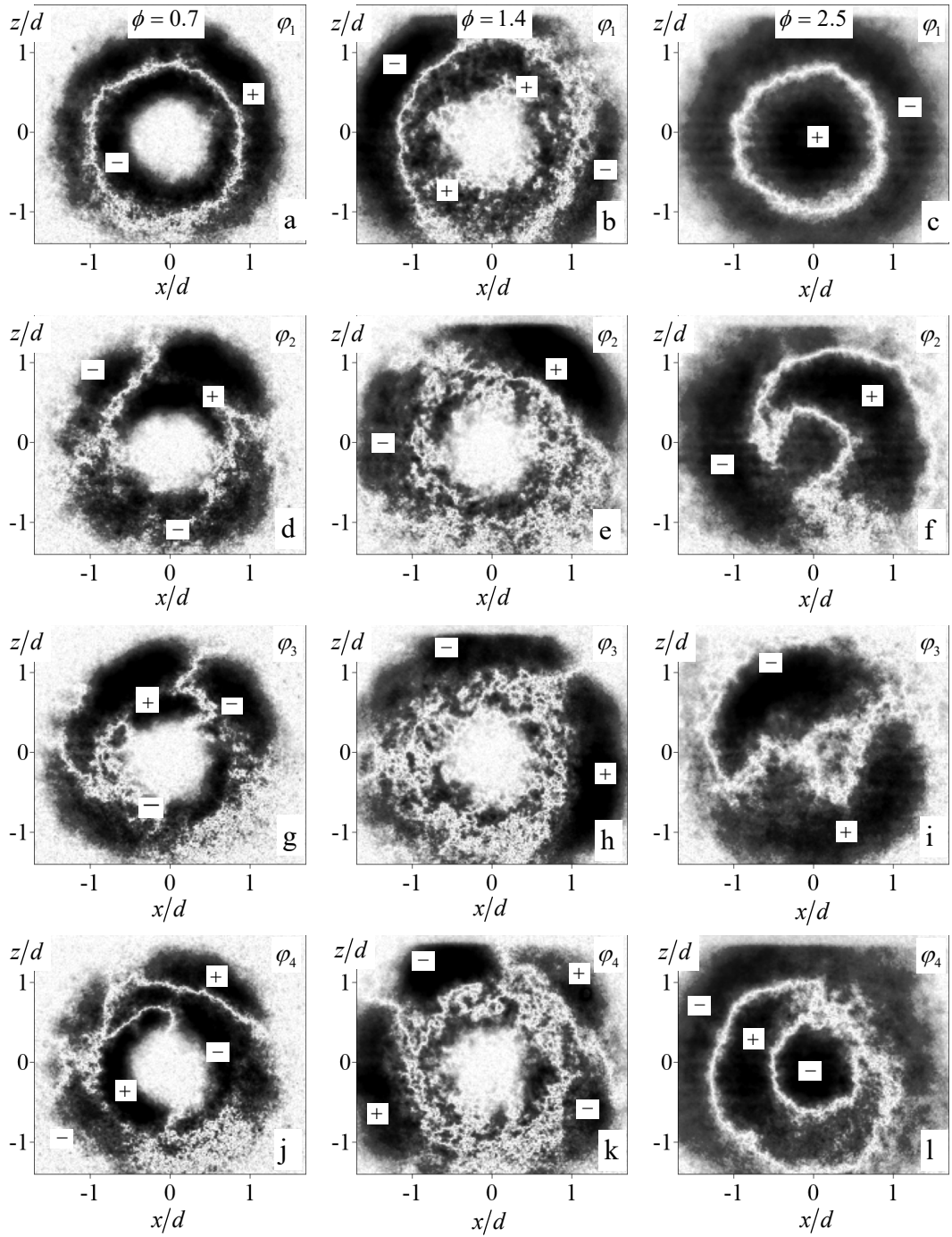


Figure 7. Spatial distributions of the first four PCA modes (a-c)  $\varphi_1$ , (d-f)  $\varphi_2$ , (g-i)  $\varphi_3$ , (j-l)  $\varphi_4$  for

PLIF data for the transverse cross-section  $y/d = 1.5$  of the swirling methane/air flames for

(a,d,g,j)  $\phi = 0.7$ , (b,e,h,k)  $\phi = 1.4$ , (c,f,i,l)  $\phi = 2.5$

## Conclusions

Experimental study of reaction zone deformations in turbulent swirling methane/air flames has been carried out by using the HCHO PLIF technique. For the fuel-lean mixture with  $\phi = 0.7$  and fuel-rich mixture with  $\phi = 1.4$  the flame shape corresponded to an inverted cone. The fuel-rich mixture ( $\phi = 2.5$ ) burned as a lifted flame, detached from the burner rim. HCHO was detected between the surrounding air and the fuel-rich jet and also at the axis. The HCHO PLIF images, captured for the transverse and longitudinal planes, were processed by principle component analysis to reveal coherent structures in deformations of the reaction zone. Two types of large-scale deformations have been observed, namely, deformations induced by almost axisymmetric mode and those caused by rotating an asymmetric coherent structure. It is concluded that the former type is caused by the buoyancy force acting between the hot combustion products and the atmospheric air. The latter type, corresponded to disturbance waves propagating along the flame front, is presumably associated with precession of a pair of large-scale helical vortex structures, detected from PIV measurements in the previous studies [1, 14].

**Acknowledgements:** This work was supported by Russian Science Foundation (grant No. 16-19-10566).

## References

- [1] **Alekseenko S. V., Dulin V. M., Kozorezov Y. S., Markovich D. M.** Effect of high-amplitude forcing on turbulent combustion intensity and vortex core precession in a strongly swirling lifted propane/air flame // *Combust. Sci. Technol.* – 2012. – V. 184, № 10-11. – P. 1862-1890.
- [2] **Gupta A. K., Lilley D. G. and Syred N.** Swirl flows. Tunbridge Wells, Kent, England, Abacus Press, 1984.
- [3] **Oberleithner K., Paschereit C. O., Seele R. and Wygnanski I.** Formation of turbulent vortex breakdown: intermittency, criticality, and global instability // *AIAA J.* – 2012. – V 50, № 7. – P. 1437-1452.
- [4] **Syred N.** A review of oscillation mechanisms and the role of the precessing vortex core (PVC) in swirl combustion systems // *Progr. Energy Combust. Sci.* – 2006. – V. 32, № 2. – P. 93-161.
- [5] **Lieuwen T.C.** Unsteady combustor physics. Cambridge University Press, 2012.
- [6] **Stöhr M., Sadanandan R., Meier W.** Phase-resolved characterization of vortex–flame interaction in a turbulent swirl flame // *Exp. Fluids.* – 2011. – V. 51, № 4. – P. 1153-1167.
- [7] **Boxx I., Stöhr M., Carter C., Meier W.** Temporally resolved planar measurements of transient phenomena in a partially pre-mixed swirl flame in a gas turbine model combustor // *Combustion and Flame.* – 2010. – V. 157, № 8. – P. 1510-1525.

[8] **Sirovich L.** Turbulence and the dynamics of coherent structures. I. Coherent structures // *Quart. Appl. Math.* – 1987. – V. 45, № 3. – P. 561-571.

[9] **Glassman I.** *Combustion*, 3rd ed. Academic Press, San Diego, 1996.

[10] **Brackmann C., Nygren J., Bai X., Li Z., Bladh H., Axelsson B., Denbratt I., Koopmans L., Bengtsson P-E., Alden M.** Laser-induced fluorescence of formaldehyde in combustion using third harmonic Nd:YAG laser excitation // *Spectrochimica Acta Part A.* – 2003. – V. 59, № 14. – P. 3347-3356.

[11] **Harrington J. E., Smyth K. C.** Laser-induced fluorescence measurements of formaldehyde in methane/air diffusion flame // *Chem. Phys. Lett.* – 1993. – V. 202, № 3-4. – P. 196-202.

[12] **Brackmann C., Li Z., Rupinski M., Docquier N., Pengloan G., Alden M.** Strategies for formaldehyde detection in flames an engines using a single-mode Nd:YAG/OPO laser system // *Appl. Spectrosc.* – 2005. – V. 59, № 6. – P. 763-768.

[13] **Kerschen G., Golinval J. C., Vakakis A. F., Bergman L. A.** The method of proper orthogonal decomposition for dynamical characterization and order reduction of mechanical systems: an overview // *Nonlin. Dyn.* – 2005. – V. 41, № 1. – P. 147-169.

[14] **Markovich D.M., Abdurakipov S.S., Chikishev L.M., Dulin V.M., Hanjalić K.** Comparative analysis of low-and high-swirl confined flames and jets by proper orthogonal and dynamic mode decompositions // *Phys. Fluids.* – 2014. – V. 26, №. 6. – 065109.